VASCULAR-INTERVENTIONAL

Maria-Katharina Ganten
Ute Krautter
Hendrik von Tengg-Kobligk
Dittmar Böckler
Hardy Schumacher
Wolfram Stiller
Stefan Delorme
Hans-Ulrich Kauczor
Günter W. Kauffmann
Michael Bock

Quantification of aortic distensibility in abdominal aortic aneurysm using ECG-gated multi-detector computed tomography

M.-K. Ganten (✉) · U. Krautter ·
H. von Tengg-Kobligk · S. Delorme ·
H.-U. Kauczor
Department of Radiology, Medical
Physics in Radiology,
Deutsches Krebsforschungszentrum,
Im Neuenheimer Feld 280,
69120 Heidelberg, Germany
e-mail: m.ganten@dkfz-heidelberg.de
Tel.: +49-6221-422493
Fax: +49-6221-422462

M.-K. Ganten · G. W. Kauffmann
Department of Diagnostic Radiology,
Ruprecht-Karls-University of Heidelberg,
Heidelberg, Germany

D. Böckler · H. Schumacher
Department of Vascular
and Endovascular Surgery,
Ruprecht-Karls-University
of Heidelberg,
Heidelberg, Germany

W. Stiller · M. Bock
Department of Medical Physics
in Radiology,
Medical Physics in Radiology,
Deutsches Krebsforschungszentrum,
Heidelberg, Germany

Abstract *Rationale and objectives:* To detect distensibility changes that might be an indicator for an increased risk of rupture, cross-sectional area changes of abdominal aortic aneurysms (AAA) have been determined using ECG-gated CT. *Materials and methods:* Distensibility measurements of the aorta were performed in 67 patients with AAA. Time-resolved images were acquired with a four detector-row CT system using a modified CT-angiography protocol. Pulsatility-related cross-sectional area changes were calculated above and at AAA level by semiautomatic segmentation; distensibility values were obtained using additional systemic blood pressure measurements. Values were compared for small Ø< 5 cm (n=44) and large Ø> 5 cm (n=23) aneurysms. *Results:* The aorta could be segmented successfully in all patients. Upstream AAA distensibility D was significantly higher than at AAA level for both groups: means *above* AAA (at AAA) $D_{above} = (1.3\pm0.8)\cdot10^{-5}$ Pa^{-1} ($D_{AAA} = (0.6\pm0.5)\cdot10^{-5}$ Pa^{-1}) t-test p_D<0.0001. Differences of the distensibility between smaller and larger aneurysms were not found to be significant. *Conclusion:* Distensibility can be measured non-invasively with ECG-gated CT. The reduction of distensibility within aneurysms compared to normal proximal aorta is subtle; the lack of difference between both small and large aneurysms suggests that this reduction occurs early in the aneurysm's development. Hence, reduced distensibility might be a predictive parameter in patients with high risk of aortic disease.

Keywords MDCT · ECG-gating · Aorta · AAA · Elasticity

Introduction

In patients with asymptomatic abdominal aortic aneurysm (AAA) the fate of any individual patient is hard to predict [1]. Increasing aortic wall stiffness with a subsequent change in the wall's capacity to withstand tension changes of the pressure peaks, as a consequence of the aortic wall elastin fiber loss, could be predictive of subsequent rupture [2, 3]. In this work aortic distensibility is evaluated with ECG-gated CT [4, 5] to investigate whether distensibility would be higher in the aneurysmatic than in a non-affected segment, as postulated by Wilson [6], or rather lower, according to our own assumption. Furthermore, the difference of distensibilities for small (<5 cm) and large (>5 cm) aneurysms was

investigated, a diameter which by current standards constitutes a major rupture risk and warrants repair.

Materials and methods

Sixty-seven consecutive patients with known infrarenal abdominal aortic aneurysm who had presented to the Department of Vascular Surgery were studied. The decision to subsequently operate or not upon a patient in this study was entirely at the discretion of the surgeons in charge. Approval of the local ethics committee and informed consent were obtained properly. Twenty-three patients presented an aneurysm diameter of less than 5 cm (mean, 3.9; ± 0.9 cm); 44 presented with aneurysms of more than 5-cm diameter (mean 5.6; ±0.6 cm). The clinical characteristics of the population collected for this study are listed in Table 1. Mean age for the patients with larger sized aneurysms was 67±9 years including 35 men and 9 women. Mean age for the patients with smaller sized aneurysms was 69±9 years including 21 men and 2 women. Mean heart rate during examination was 67±12 bpm; no medication was used to reduce the heart rate during the examination.

Data acquisition

Examinations were performed using a four detector-row CT system (SOMATOM Volume Zoom; Siemens Medical Solutions, Erlangen, Germany). To reconstruct time-resolved CT data, separate retrospective ECG-gating was added to our standard CT angiography protocol. There was no adaptation of dose to morphology for the individual patient. Each patient's DLP (dose length product) is registered routinely. The acquired raw data set was used to obtain two image sets. First, standard angiography images without ECG synchronization were calculated. Second, time-resolved images were obtained with an ECG-gating algorithm developed for separate image reconstruction [4, 7] because at the time of the study no multi-phasic image reconstruction algorithm with sufficient temporal resolution was commercially avail-

able. Temporal resolution depends on the number of rotations used for interpolation, heart rate and the scanner's rotation time [4, 8], [9]. For an interpolation range of four rotations, i.e., a 2-s time window, as used in this study, data from four consecutive rotations were used. The temporal window that corresponded to this range depended on the heart rate: for example, a heart rate of 60 bpm to the window was two heart beats long. In this study the temporal resolution ranged between 90 and 250 ms. The patient's abdomen was scanned after an i.v. pump infusion of 130 ml Iomeprol 300 (Imeron, Altana Pharma, Konstanz, Germany) at a flow rate of 4 ml/s. The automated bolus tracking program implemented on the scanner was applied, and a ROI was placed in the abdominal aorta using a threshold of 110 HU.

The scans of the four detector-row CT scanner covered the whole abdomen and were performed with a rotation time of 0.5 s at 120 kV peak voltage, a current-time product of 120 mAs (effective), a pitch of 0.375, an acquisition slice thickness of 2.5 mm and thus a collimation of 10 mm (i.e., 4×2.5 mm). Reconstruction thickness was 2.5 mm. A collimation of 10 mm (4×2.5 mm) was used to cover the whole examination region within an image acquisition time of about 30 s and thus to acquire all images during a single breath hold period. The protocol was the same as our standard CT-angiography protocol.

From the so derived data set, 20 time frames per heart cycle were calculated at each position, i.e., images were reconstructed at 0%, 5%, 15%...95% of the RR interval by half scan reconstructions. This temporal resolution is required to define the phases of minimum and maximum aortic distension. Aortic cross-sectional area changes were determined at two positions of the aorta, immediately above the infrarenal AAA and at the level of its maximal diameter (Fig. 1). The positions were selected by a senior radiologist experienced in vascular CT.

In order to exclude major subclavian artery stenosis, bilateral brachial arterial blood pressure was registered non-invasively using an arm cuff before examination. Directly after image acquisition unilateral blood pressure was registered for distensibility calculation. To minimize

Table 1 Patients' clinical characteristics

	All subjects, n=67	Ø>5 cm, n=44	Ø=5 cm, n=23
Gender ratio (male:female)	56:11	40:4	16:7
Mean age (range; ±SD) [years]_	68 (43–89; ±9)	69 (44–89; ±9)	66 (43–85; ±9)
Body mass index (range; ±SD) [kg/m^2]	27.0 (19.2–35.5; ±3.2)	26.9 (19.3–35.5; ±3.5)	27.1 (21.2–33.8; ±2.8)
Smokers	26	21	5
Diabetes	15	9	6
Systolic blood pressure [mmHg]	145±20	143±20	145±20
Diastolic blood pressure [mmHg]	82±17	84±31	81±10
Mean of maximal aortc diameter (±SD) [cm]	4.8 (±1.3)	6.0 (±0.8)	4.0 (±0.8)

Fig. 1 Surface reconstruction of the CTA data showing the two positions above the branching of the renal arteries and at the level of the aneurysm (AAA) for functional image reconstruction indicated as horizontal lines (**a**) in a patient presenting a small aneurysm, (**b**) in a patient presenting a big aneurysm
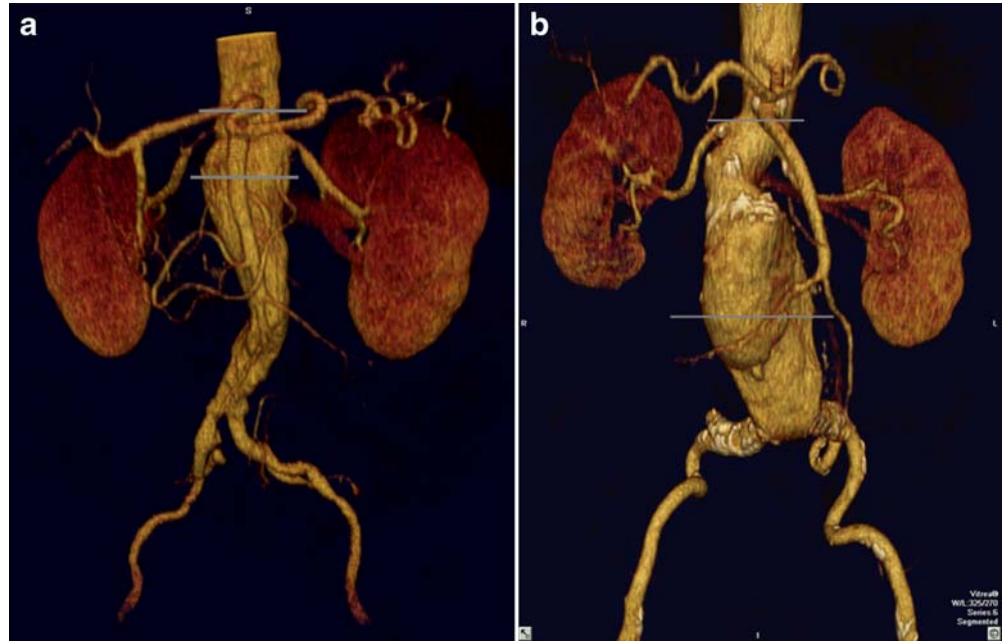
the error in pressure estimation, an automatic pneumatic sphygmanometer was used (Maglife C, Schiller Medical SA, Wissembourg, France). The measurement accuracy of this system as given by the manufacturer is 2%.

Determination of vessel area

The vessel area was determined from the ECG-gated time-resolved image series of 20 images. Because of the high degree of operator-dependence with manual outlining of the aortic wall area, we preferred to use a semi-automatic segmentation algorithm, which detected the arterial wall in all CT images of the cardiac cycle. The algorithm has been described in the literature [10, 11] and tested previously [12]. Briefly, a seed point was defined near the center of the aorta. Next, the algorithm inflated a so-called active contour starting at the seed point like a balloon until the vessel wall was found. In order to better fit the boundary, the final contour was refined by an iterative process (Figs. 2 and 3).

Elasticity quantification

The visco-elastic properties of the aortic wall are typically characterized by two parameters: dilation d [mm] and distensibility D [pa^{-1}]. The dilation is defined as the maximum systolic-to-diastolic diameter change of the selected area [13]:

$$d = d_{sys} - d_{dia} \tag{1}$$

Distensibility D [pa^{-1}] is defined as the relative change in vessel cross-sectional area A [mm^2] that occurs during the cardiac cycle, divided by the corresponding change in blood pressure Δp [Pa].

$$D = \frac{\Delta A}{A_0 \cdot \Delta p} \tag{2}$$

A_0 is the minimum vessel area over the cardiac cycle, and ΔA is the difference between maximum and minimum area [14]; Δp can be estimated using sphygmomanometry [15].

In order to compare results with literature values, distensibility was also converted into pulse wave velocity PWV [m/s] [14]:

$$PWV = \frac{1}{\sqrt{D \cdot \rho}} \tag{3}$$

Here $\rho = 1055 \cdot 10^3$ [kg/m^3] denotes the mass density of blood that is assumed to be constant.

For each time series the segmentation process was repeated five times, and the reproducibility coefficient of variation was determined. Distensibility values were calculated using Eq. 2. Paired t-test was performed to assess the statistical significance of differences at the AAA level and adjacent aorta; difference between large and small aneurysms were tested by t-test with SAS software (version 9.1; SAS Institute Inc., Cary, NC). Box plots were generated using R software (version 2.4.1. The R Foundation for Statistical Computing).
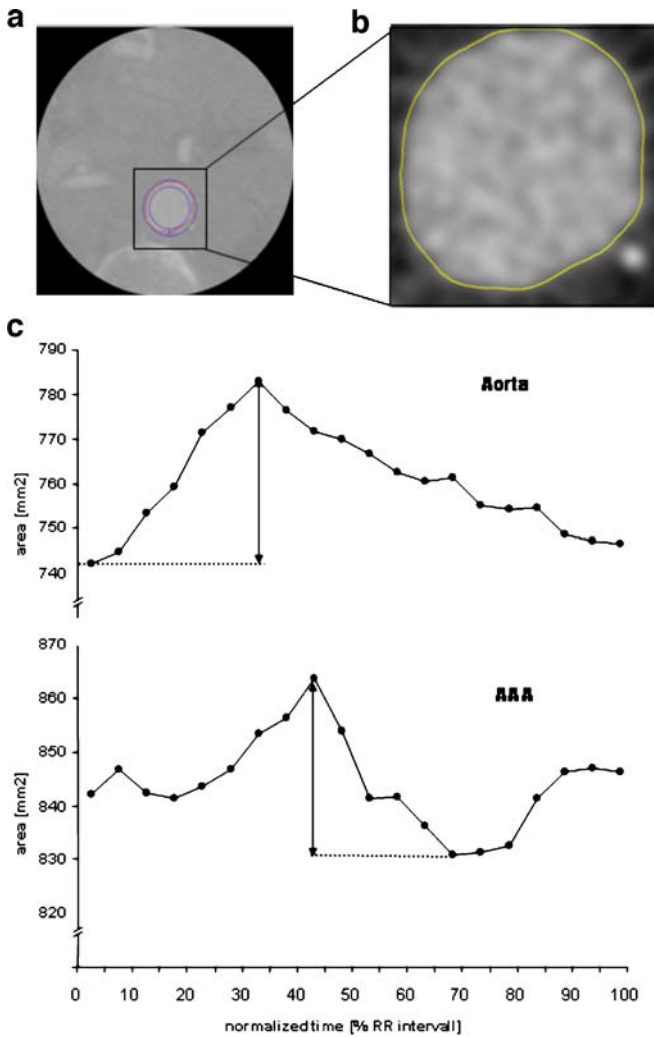
Fig. 2 Illustration of the processing steps required to calculate the vessel area. The example shows a single time frame of the functional images aortic diameter <5 cm of the patient presented in Fig. 1a (**a**) of the suprarenal aorta. The CT images are segmented using an active contour algorithm, setting a seed point and defining two ROIs in between which the vessel wall is found (**b**). The resulting area-versus-time curve (in percent of RR interval) is shown for the patient's area change in the aorta and at the level of aneurysm AAA (**c**)

Results

With the active contour algorithm the cross-sections of the aorta could be segmented successfully in all 67 patients (Fig. 2), although some minor streak artifacts were visible due to the limited amount of data for reconstruction. Mean signal variation on the streak artifacts was on the order of 32 HU. Difference in density between the vessel lumen and the surrounding fatty tissue was 297 HU. Coefficient of variation for the five measurements in each patient was 8.6%. The mean patient DLP (dose length product) was 900±232 mGy x cm for the two helicals (native, arterial ECG-gated contrast phases). $CTDI_w$ for the applied protocol was $CTDIw=41$ mGy.

Distensibility, pulse wave velocity values and dilation were calculated (Tables 2, 3, 4). A significant difference in distensibility D (dilation d) between the adjacent aorta wall and the aneurysm was found for both aneurysm sizes. Upstream (AAA) means for both groups together were $D_{above}=(1.3\pm0.8)\cdot[10^{-5}\ Pa^{-1}]$, $D_{AAA}=(0.6\pm0.5)\cdot[10^{-5}\ Pa^{-1}]$, t-test large AAA: $p_D<0.0001$, ($p_d=0.04$) and t-test small AAA: $p_D<0.0001$, ($p_d=0.045$) visualized in the box plot in Fig. 4.

However differences between large and small AAA were not found to be significant. Distensibility values were very low for both groups. The upstream AAA distensibility range for both groups was $D=(0.4–3.7)\ [10Pa^{-1}]$. At AAA the range was $D=(0.1–3.6)\ [10Pa^{-1}]$. This corresponds to a pulse wave velocity (PWV) range of above AAA level PWV= (5.1–15.9) m/s and at AAA level of PWV=(5.1 to 29.9) m/s. Likewise dilation was very small at the AAA with a range of (0.1–2.8) mm and slightly higher above the AAA with a range of (0.4–2.5–29.9) mm.

Discussion

The main characteristic of an abdominal aortic aneurysm (AAA) is the replacement of the medial elastic fibers by connective tissue, with a loss of elastic properties, increase in diameter and, finally, wall rupture. Other factors, such as parietal calcification, intrasaccular thrombus and maximum diameter, may possibly modify the behavior of the aortic wall. Thus, distensibility might provide information about the constitution of the arterial wall.

Several techniques have been proposed to measure vascular distensibility non-invasively: These include pulse-wave velocity measurements employing either magnetic resonance velocity mapping [15–18], or Doppler ultrasound [19], and methods that monitor the change of the vessel cross-sectional area during the cardiac cycle [20]. From the change in cross-sectional area between systole and diastole and an estimate of the corresponding intra-arterial pressure difference, the distensibility can be calculated. The latter has been done using magnetic resonance imaging [21, 22] and ultrasound [20, 23]. Ultrasound image data cannot image all parts of the aorta in a single view. MR pulse wave velocity measurements are unreliable in situations with complex flow patterns [24]; availability of MR systems is limited, the acquisition of several pulse sequences prolongs scan time, and monitoring of instable patients can be difficult. Finally, spatial resolution of MRI is currently inferior to that of CT. Therefore, in spite the radiation exposure, CT angiography still is the preferred method to screen aortic pathologies [25–27].

In this study, the distensibility was assessed indirectly by measurement of the change over time of the vessel cross-sectional area, using ECG-gated MDCT and by measuring

Fig. 3 Processing steps required to calculate vessel area, shown for an example measurement at aneurysm level Ø<5 cm. The example shows the functional image (**a**) of the aneurysmatic aorta of the patient presented in Fig. 1b. The reconstructed CT images are segmented using the active contour algorithm, setting a seed point and defining two ROIs in between which the vessel wall is found (**b**). The resulting area-versus-time curve (in percent of RR interval) is shown for the patient's area change at the AAA (**c**)
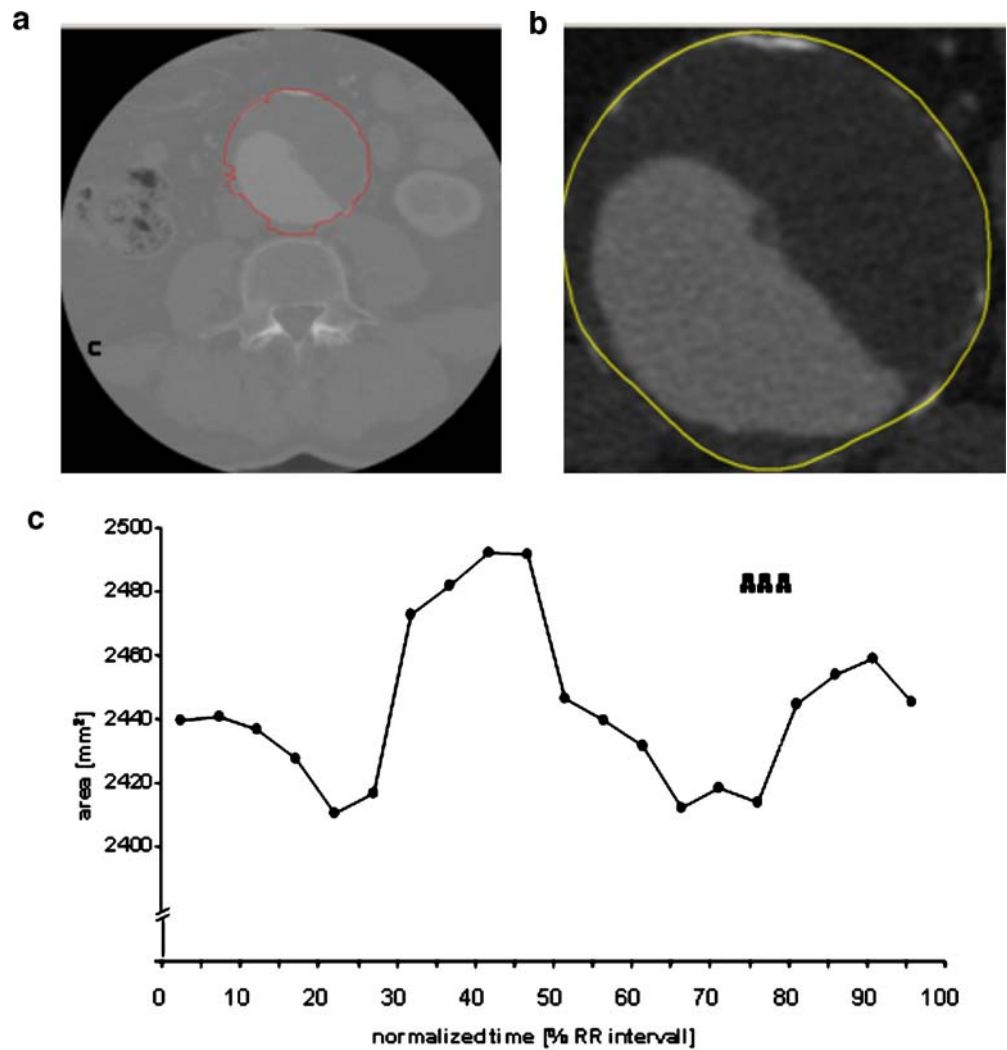
peripheral systemic blood pressure. The vessel cross-sectional area was determined from CT image data by a semiautomatic segmentation algorithm in AAA patients. It was tested whether substantial distensibility changes can be found above the AAA vs. AAA level for two aneurysm sizes, since smaller aneurysms are known to be less likely to rupture than larger aneurysms. The technique applied in

Table 2 Distensibility of small vs. large aneurysms

	D [10^{-5} Pa^{-1}] all subjects	D [10^{-5} Pa^{-1}] Ø≤5 cm	D [10^{-5} Pa^{-1}] Ø>5 cm
Above aneurysm	1.30±0.8	1.12±0.6	1.41±0.9
At aneurysm	0.6±0.5	0.56±0.4	0.69±0.6
P value*	p<0.0001	p<0.0001	p<0.0001

*P value is given for the difference in distensibility between the values above aneurysm vs. AAA level

this study has already been validated to derive cyclic cross-sectional area changes of the aorta [4, 28] and tested on angiography data sets from patients undergoing routine MDCT [29].

We found that the distensibility D was significantly lower in the aneurysms than in the proximal, non-aneurysmatic parts of the aorta and that there was no apparent difference between small and larger aneurysms. This finding supports our hypothesis that the normal vessel is more distensible and can better withstand systemic pressure peaks, whereas the wall of the AAA is stiffer. We believe that this is a plausible explanation for the pathomechanism that ultimately leads to an aneurysm in this area, since in a stiffened vessel wall, the impact of distending forces is more likely to cause damage than in a compliant wall.

The results did not show any statistical difference in aneurysmal aortic wall mechanics in AAAs with a diameter of more than 5 cm vs. smaller aneurysms, which are generally treated conservatively. The number of individuals

Table 3 Results-pulse wave velocity of small vs. large aneurysms

	PWV [m·s^{-1}] all subject	PWV [m·s^{-1}] Ø≤5 cm	PWV [m·s^{-1}] Ø>5 cm
Above aneurysm	9.55±2.6	9.96±2.6	9.33±2.6
At aneurysm	15.08±5.5	15.39±5.3	14.92±5.7
P value*	p<0.0001	p<0.0001	p<0.0001

*P value is given for the difference in pulse wave velocity between the values above aneurysm vs. AAA level

with aneurysms of less than 5 cm was quite small (n=23), which makes it difficult to rule out smaller differences between the groups.

The time-resolved images show streak artifacts that lead to artificial contour changes using the described algorithm. This systematic error fundamentally limits the achievable precision in the distensibility calculations. Streak artifacts will simulate vessel dilation in completely stiffened vessels.

Indirect measurement of arterial blood pressure may lead to a small systematic error of the obtained pressure values. However, in patient studies this error is consistent [30]. Furthermore, invasive blood pressure measurements would not be practicable in patients undergoing routine CT examinations.

In a recent study, an age-dependent loss of distensibility was found in patients without known vascular diseases, using the same method [29]. Averaging over all of our patients with aneurysm yielded a low mean distensibility: D=1.35 10^{-5} Pa^{-1} above and D=0.65 10^{-5} Pa^{-1} at the aneurysm level, whereas the expected distensibility (according to extrapolation of the literature data) for a 68.5-year-old human, representing the mean age group, not suffering from abdominal aorta aneurysm would have been D=1.9 10^{-5} Pa^{-1} above and D=1.06 10^{-5} Pa^{-1} below the renal arteries.

The pitch used in this study is not small enough for cardiac imaging; however, for aortic vessel area determination a lower temporal resolution is acceptable if a certain temporal smearing of the data is tolerated. To measure the maximum and minimum vessel area the exact temporal correlation within the heart cycle is not required, because the changes do not occur as rapidly as in the heart. Although low pitch values are necessary to reconstruct time-resolved images, relatively high pitch values of 0.375 were used here to limit radiation dose. These pitch values

Table 4 Results-dilation of small vs. large aneurysms

	d [mm] all subjects	d [mm] Ø = 5 cm	d [mm] Ø> 5 cm
Above aneurysm	1.8±09	1.6±0.8	1.9±1
At aneurysm	1.5±0.8	1.2±0.6	1.6±0.9
P value*	p<0.045	p<0.045	p<0.040

*P value is given for the difference in dilation between the values above aneurysm vs. AAA level
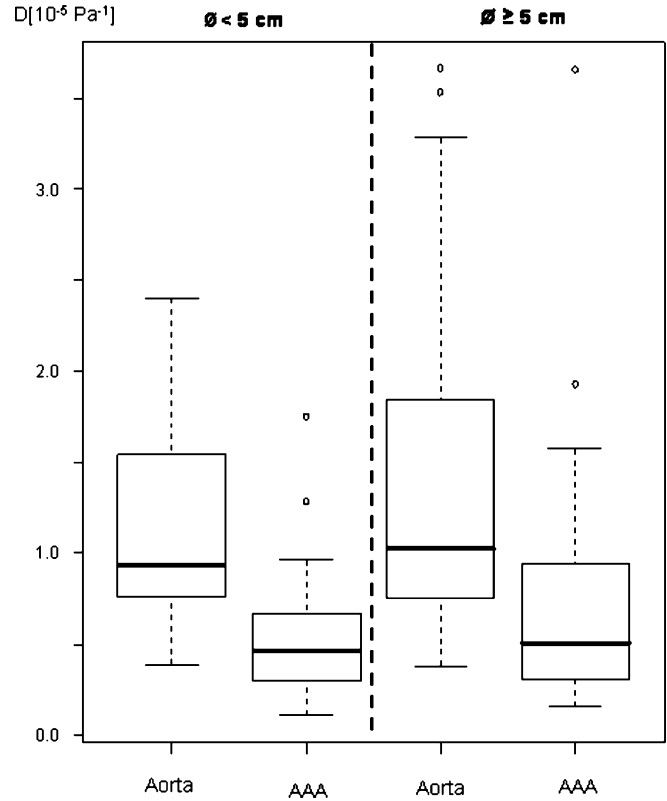

Fig. 4 Box plot: Comparison of the distensibilities in the aorta and at aneurysm level (AAA) for small and big aneurysm. The box stretches from the lower hinge (defined as the 25th percentile) to the upper hinge (the 75th percentile). The median is shown as a line across the box. The "H-spread" is defined as the difference between the hinges, and a "step" is defined as 1.5 times the H-spread. Inner fences are one step beyond the hinges. Outer fences are two steps beyond the hinges. There are two adjacent values: the largest value below the upper inner fence and the smallest value above the lower inner fence. For the data plotted in the figure, the minimum value is above the upper inner fence and is therefore the lower adjacent value. The maximum value is the inner fences so it is not the upper adjacent value. As shown in the figure, a line is drawn from the upper hinge to the upper adjacent value and from the lower hinge to the lower adjacent value. Every score between the inner and outer fences is indicated by an "o"

correspond to our routine non ECG-gated CT angiography protocol. With the mean DLP of 900±232 mGy x cm (dose length product) for the two helicals (native, arterial ECG-gated contrast phases), this scan protocol did not exceed the diagnostic reference value given by the German Federal Radiation Protection Authority for abdominal scan protocols, where a DLP of 1,500 mGy x cm for 2.5 helicals is indicated [31].

In this study arterial wall distensiblity was assessed in AAA patients by ECG-gated CT angiography. As CT angiography is routinely performed for many aortic diseases, the presented method can be integrated into a clinical protocol. The small additional effort is appropriate for routine clinical use. The image protocol provides correct morphological as well as functional information about the

vessel distensibility. With a semiautomatic segmentation algorithm, vessel cross-sectional area was measured. Further improvements of the segmentation algorithm will facilitate the determination of distensibility as a by-product of CT angiography. Thus, the proposed method will benefit from the ongoing improvements in CT technology [32].

In the literature it is controversial whether a difference in aortic wall mechanics indicates those AAAs that subsequently rupture. Wilson et al. [6] applied an ultrasound B-mode echo-tracking device and found that baseline AAA compliance was significantly related to rupture. He also hypothesized that aneurysms with low stiffness are the ones with risk of rupture [33], whereas Moritake et al. hypothesized that the stiffest aneurysms might be the ones most prone to rupture [34]. Sonesson et al. [35] as well as Mac Sweeney et al. [3] so far failed to show any relationship between the stiffness of aneurysms and their size, which is in agreement with our results. Possibly the loss of elastic properties precedes the formation of the aneurysms, so that, once this has happened, the ensuing changes are only destructive ones, resulting in further dilatation, ultimately rupture, but only minimal alterations of the already deteriorated elastic properties. So far, we remain unable to determine the signs that herald an imminent rupture of an aneurym. However, stiffening of an aortic wall that otherwise appears to be normal, with respect to the patient's age, might be a sign that this vessel is at risk of developing an aneurism in the future.

Conclusion

It is possible to determine distensibility non-invasively with ECG-gated CT of abdominal aortic aneurysms. The normal vessel is more distensible and can better withstand systemic pressure peaks, whereas the wall of the AAA is stiffer. However, reduction of distensibility within aneurysms compared to normal proximal aorta is subtle; the lack of difference between both small and large aortic aneurysms suggests that this reduction occurs early in the aortic aneurysm's development. Hence reduced aortic distensibility might be a predictive parameter in patients with high risk of aortic disease, e.g., diabetes mellitus or Marfan's syndrome.

References

1. Stonebridge PA, Draper T, Kelman J et al (1996) Growth rate of infrarenal aortic aneurysms. Eur J Vasc Endovasc Surg 11(1):70–73
2. MacSweeney ST, Powell JT, Greenhalgh RM (1994) Pathogenesis of abdominal aortic aneurysm. Br J Surg 81(7):935–941
3. MacSweeney ST, Young G, Greenhalgh RM et al (1992) Mechanical properties of the aneurysmal aorta. Br J Surg 79(12):1281–1284
4. Ganten M, Boese JM, Leitermann D et al (2005) Quantification of aortic elasticity: development and experimental validation of a method using computed tomography. Eur Radiol 15(12):2506–2512
5. Teutelink A, Rutten A, Muhs BE et al (2006) Pilot study of dynamic cine CT angiography for the evaluation of abdominal aortic aneurysms: implications for endograft treatment. J Endovasc Ther 13(2):139–144
6. Wilson KA, Lee AJ, Hoskins PR et al (2003) The relationship between aortic wall distensibility and rupture of infrarenal abdominal aortic aneurysm. J Vasc Surg 37(1):112–117
7. Boese JM, Bahner ML, Albers J et al (2000) [Optimizing temporal resolution in CT with retrospective ECG gating]. Radiologe 40(2):123–129
8. Boese JM, Bahner ML, Albers J et al (2001) An improved algorithm for multi-slice cardiac CT imaging with high temporal resolution (abstr). Radiology 221(P):457
9. Kachelriess M, Ulzheimer S, Kalender WA (2000) ECG-correlated image reconstruction from subsecond multi-slice spiral CT scans of the heart. Med Phys 27(8):1881–1902
10. Lobregt S, Viergever MA (1995) A discrete dynamic contour model. Trans Med Imaging 14:12–24
11. Cohen L (1991) On active contour modelsand ballons. Image understanding 53:211–218
12. Krug R, Boese JM, Schad LR (2003) Determination of aortic compliance from magnetic resonance images using an automatic active contour model. Phys Med Biol 48(15):2391–2404
13. Malina M, Lanne T, Ivancev K et al (1998) Reduced pulsatile wall motion of abdominal aortic aneurysms after endovascular repair. J Vasc Surg 27(4):624–631
14. Nichols WW (1990) Properties of the arterial wall. In: Nichols WW, O' Rourke MF (eds). McDonald's Blood flow in arteries. Edward Arnold, London, p 96
15. Nollen GJ, Westerhof BE, Groenink M et al (2004) Aortic pressure-area relation in Marfan patients with and without beta blocking agents: a new non-invasive approach. Heart 90(3):314–318
16. Boese JM, Bock M, Schoenberg SO et al (2000) Estimation of aortic compliance using magnetic resonance pulse wave velocity measurement. Phys Med Biol 45(6):1703–1713
17. Kraft KA, Itskovich VV, Fei DY (2001) Rapid measurement of aortic wave velocity: in vivo evaluation. Magn Reson Med 46(1):95–102
18. Bock M, Schad LR, Muller E et al (1995) Pulsewave velocity measurement using a new real-time MR-method. Magn Reson Imaging 13(1):21–29
19. Long A, Rouet L, Bissery A et al (2004) Compliance of abdominal aortic aneurysms: evaluation of tissue Doppler imaging. Ultrasound Med Biol 30(9):1099–108

20. Long A, Rouet L, Bissery A et al (2004) Aortic compliance in healthy subjects: evaluation of tissue Doppler imaging. Ultrasound Med Biol 30 (6):753–759

21. Mohiaddin RH, Yang GZ, Burger P et al (1992) Automatic enhancement, animation, and segmentation of flow in peripheral arteries from MR phase-shift velocity mapping. J Comput Assist Tomogr 16(2):176–181

22. Lalande A, Khau van Kien P, Salve N et al (2002) Automatic determination of aortic compliance with cine-magnetic resonance imaging: an application of fuzzy logic theory. Invest Radiol 37 (12):685–691

23. Wilson KA, Hoskins PR, Lee AJ et al (2000) Ultrasonic measurement of abdominal aortic aneurysm wall compliance: a reproducibility study. J Vasc Surg 31(3):507–513

24. Erbel R, Alfonso F, Boileau C et al (2001) Diagnosis and management of aortic dissection. Eur Heart J 22 (18):1642–1681

25. Hahmann M, Richter GM, Schuhmacher H et al (2001) [Post-traumatic dissection of the abdominal aorta]. Radiologe 41(7):590–594

26. Hansmann HJ, Dobert N, Kucherer H et al (2000) Various spiral CT protocols and their significance in the diagnosis of aortic dissections: results of a prospective study. Rofo 172(11):879–887

27. Ockert S, Bockler D, Ganten M et al (2006) Images in vascular medicine. Persistent sac enlargement after conventional replacement of an inflammatory aortic aneurysm. Vasc Med 11 (2):131–132

28. Hahmann M, Boese JM, Leitermann D et al (2001) Measurement of aortic elasticity using ECG-gated multidetector-row CT: An ex-vivo experiment (abstr.). Radiology 221(P):33

29. Ganten M, Krautter U, Hosch W et al (2007) Age related changes of human aortic distensibility: evaluation with ECG-gated CT. Eur Radiol 17(3):701–708

30. Imura T, Yamamoto K, Kanamori K et al (1986) Non-invasive ultrasonic measurement of the elastic properties of the human abdominal aorta. Cardiovasc Res 20(3):208–214

31. Bundesamt für Strahlenschutz B (2003) Bekanntmachung der diagnostischen Referenzwere für radiologische und nuklearmedizinische Untersuchungen. Bundesanzeiger Nr 143 (Tab. 3):17503

32. Wintersperger B, Jakobs T, Herzog P et al (2005) Aorto-iliac multidetector-row CT angiography with low kV settings: improved vessel enhancement and simultaneous reduction of radiation dose. Eur Radiol 15(2):334–341

33. Wilson K, Bradbury A, Whyman M et al (1998) Relationship between abdominal aortic aneurysm wall compliance and clinical outcome: a preliminary analysis. Eur J Vasc Endovasc Surg 15(6):472–477

34. Moritake K, Handa H, Okumura A et al (1974) Stiffness of cerebral arteries-its role in the pathogenesis of cerebral aneurysms. Neurol Med Chir (Tokyo) 14 pt 1:47–53

35. Sonesson B, Sandgren T, Lanne T (1999) Abdominal aortic aneurysm wall mechanics and their relation to risk of rupture. Eur J Vasc Endovasc Surg. 18(6):487–493